Published in final edited form as:
Exp Cell Res. 2015 February 15; 331(2): 292–308. doi:10.1016/j.yexcr.2014.09.032.

Intercellular Adhesion Molecule-1 Expression by Skeletal Muscle Cells Augments Myogenesis

Qingnian Goh[1], **Christopher L. Dearth**[1], **Jacob T. Corbett**[1], **Philippe Pierre**[3,4,5], **Deborah N. Chadee**[2], and **Francis X. Pizza**[1]

[1]Department of Kinesiology, The University of Toledo, Toledo, Ohio

[2]Department of Biological Sciences, The University of Toledo, Toledo, Ohio

[3]Centre d'Immunologie de Marseille-Luminy U2M, Aix-Marseille Université, Marseille, France

[4]INSERM U631, Institut National de la Santé et Recherche Médicale, Marseille, France

[5]CNRS UMR6102, Centre National de la Recherche Scientifique, Marseille, France

Abstract

We previously demonstrated that the expression of intercellular adhesion molecule-1 (ICAM-1) by skeletal muscle cells after muscle overload contributes to ensuing regenerative and hypertrophic processes in skeletal muscle. The objective of the present study is to reveal mechanisms through which skeletal muscle cell expression of ICAM-1 augments regenerative and hypertrophic processes of myogenesis. This was accomplished by genetically engineering C2C12 myoblasts to stably express ICAM-1, and by inhibiting the adhesive and signaling functions of ICAM-1 through the use of a neutralizing antibody or cell penetrating peptide, respectively. Expression of ICAM-1 by cultured skeletal muscle cells augmented myoblast-myoblast adhesion, myotube formation, myonuclear number, myotube alignment, myotube-myotube fusion, and myotube size without influencing the ability of myoblasts to proliferate or differentiate. ICAM-1 augmented myotube formation, myonuclear accretion, and myotube alignment through a mechanism involving adhesion-induced activation of ICAM-1 signaling, as these dependent measures were reduced via antibody and peptide inhibition of ICAM-1. The adhesive and signaling functions of ICAM-1 also facilitated myotube hypertrophy through a mechanism involving myotube-myotube fusion, protein synthesis, and Akt/p70s6k signaling. Our findings demonstrate that ICAM-1

Correspondence: Francis X. Pizza, Ph.D., Dept. of Kinesiology, The University of Toledo, 2801 W. Bancroft St., Toledo, OH 43606, Phone: 419-530-4178, FAX: 419-530-4759, Francis.Pizza@utoledo.edu.

Competing Interests
The authors declare there are no competing financial or non-financial interests.

Authors Contribution
QG participated in study design, acquisition of multiple data sets, analysis and interpretation of data, and writing the manuscript, CLD participated in study design, creation of stable cell lines, acquisition of data, and analysis and interpretation of data, JTC assisted in image analysis, PP provided puromycin antibody, DNC participated in study design and interpretation of p38 MAPK data, FXP conceived of the study, and participated in data collection, analysis, and interpretation, as well as writing the manuscript. All authors read and approved the final manuscript.

expression by skeletal muscle cells augments myogenesis, and establish a novel mechanism through which the inflammatory response facilitates growth processes in skeletal muscle.

Keywords

Inflammation; adhesion molecules; muscle regeneration; muscle hypertrophy

Introduction

Cellular and molecular processes associated with the development of muscular tissue (myogenesis) serve to restore structure and function to skeletal muscle injured by exercise, trauma, or disease, as well as facilitate muscle hypertrophy after mechanical loading (e.g., muscle overload). Myogenesis is preceded by the proliferation of a specialized population of myogenic stem cells known as satellite cells, which normally reside in a quiescent state between the sarcolemma and the basal lamina of myofibers, leading to an increased number of muscle precursor cells (myoblasts) in skeletal muscle [1]. In the initial stage of myogenesis, myoblasts differentiate, adhere to each other, and fuse to form multinucleated myotubes [2–6]. Nascent myotubes add nuclei and hypertrophy through the fusion of myoblasts with myotubes, myotube-myotube fusion, and increased protein synthesis [2–7]. In adult muscle, muscle injury recapitulates some aspects of developmental myogenesis as indicated by the formation and maturation of centrally nucleated (regenerating) myofibers, which reflect myotube formation and their subsequent hypertrophy into normal myofibers with peripherally located nuclei [2]. These newly formed myofibers restore muscle structure and function by replacing necrotic myofibers within injured muscle. Satellite cell/myoblast proliferation and regenerating myofibers have also been observed in hypertrophying muscles after muscle overload [8–12]. The extent to which satellite cells and regenerating myofibers contribute to overload-induced hypertrophy remains controversial [11, 12].

We previously reported that adhesion molecules of the inflammatory response, such as leukocyte specific β2 integrins and intercellular adhesion molecule-1 (ICAM-1;CD54), contribute to the regulation of regenerative and hypertrophic processes in skeletal muscle [9, 10, 13]. ICAM-1 is a membrane glycoprotein consisting of an extracellular domain, a transmembrane segment, and a short cytoplasmic domain. The extracellular domain of ICAM-1 functions as a ligand for α-subunits of β2 integrins (CD11a and CD11b) and fibrinogen, and ligation of ICAM-1 transduces an intracellular signal through the interaction of its cytoplasmic domain with adaptor and other cytoskeletal proteins [14, 15]. Prior work has established that ICAM-1 is not constitutively expressed by skeletal muscle cells *in vitro* or *in vivo* [10, 16, 17]. In contrast, we found ICAM-1 on the membrane of satellite cells/myoblasts, regenerating myofibers, and normal myofibers after muscle overload [10]. Expression of ICAM-1 by skeletal muscle cells and other cell types (e.g., endothelial cells and leukocytes) contributed to regenerative and hypertrophic processes in skeletal muscle, as indicated by an attenuation in regenerating myofiber formation, protein synthesis, and hypertrophy in overloaded muscles of ICAM-1−/− compared to wild type mice [10]. As the extracellular domain of ICAM-1 facilitates cell-to-cell adhesion, and the cytoplasmic domain of ICAM-1 can activate signaling pathways (e.g., p38 MAPK and Akt) [14, 15] that

are pertinent to muscle growth, we speculate that the expression of ICAM-1 by skeletal muscle cells augments myogenic processes critical to muscle regeneration and hypertrophy.

The objective of the present study was to test the hypothesis that the expression of ICAM-1 by skeletal muscle cells augments regenerative and hypertrophic processes of myogenesis. We report that ICAM-1 expression by cultured skeletal muscle cells (C2C12 cells) augmented events of myogenesis in which myotubes are forming, adding nuclei, aligning, fusing, synthesizing proteins, and hypertrophying. We also explored the involvement of the extracellular and cytoplasmic domains of ICAM-1, as well as p38 MAPK and Akt/p70s6k signaling, as mechanisms through which ICAM-1 expression by skeletal muscle cells augmented events of myogenesis.

Materials and Methods

Stable Transfections

C2C12 myoblasts (ATCC) were stably transfected with an expression vector containing murine ICAM-1 under transcriptional regulation of the human β-actin promoter (pHβA-ICAM1; kindly provided by Dr. Stephen Hedrick at The University of California, San Diego; ICAM-1+ cells) [18]. Another population of C2C12 myoblasts were stably transfected with an empty pHβAPr-1 vector (generously provided by Dr. Peter Gunning at the University of New South Wales; EV cells) [19]. Transfection quality plasmid DNA was prepared using a commercially available kit (Qiagen) and transfected using Lipofectamine™ 2000 according to the manufacturer's protocol (Life Technologies). Cells transfected with the ICAM-1 plasmid or empty vector were placed under G418 (800 μg/ml) selection for a total of 24 d to create a population of stably transfected cells. Non-transfected C2C12 myoblasts served as control cells.

Transfection efficiency was assessed via flow cytometry, western blotting, and immunofluorescence. For flow cytometry, cells were detached from tissue culture dishes using enzyme free cell disassociation buffer (Life Technologies), treated with Fc Block™ (BD Biosciences), and incubated for 30 min with a phycoerythrin (PE)-conjugated anti-ICAM-1 antibody (clone YN1/7.4) or an equivalent amount of a isotype control antibody (eBiosciences). Cells were analyzed using FACSCalibur (BD Biosciences) at the University of Toledo Flow Cytometry Core Facility using standard procedures. Western blot and immunofluorescence detection of ICAM-1 were performed as described below.

Cell Cultures

Myoblasts (control, EV, or ICAM-1+) were seeded in 24 well plates for proliferating cultures (2,500 cells/cm^2), and in 6 or 12 well plates or 100 mm dishes for differentiating cultures (5,000 cells/cm^2). Cells proliferated in Dulbecco's modified eagle medium (DMEM; Thermo Scientific) containing 10% fetal bovine serum (Sigma-Aldrich; growth medium) for up to 4 d. Upon reaching 90% confluence, cells were treated with DMEM containing 2% horse serum (Sigma-Aldrich; differentiation medium) for up to 6 d. To explore the possibility that components of horse serum influenced ICAM-1 mediated myogenesis, we also differentiated ICAM-1+ cells in DMEM supplemented with insulin (5

μg/ml), transferrin (5 μg/ml) and selenium (5 ng/ml) (ITS medium; Sigma-Aldrich). All media contained antibiotic-antimycotic reagents (100 U/ml penicillin, 0.1 mg/ml streptomycin, and 0.25 μg/ml of amphotericin B; Sigma-Aldrich) and were changed either daily (ITS medium) or every 2 d (growth and differentiation medium).

Antibody Neutralization of ICAM-1

The involvement of the extracellular domain of ICAM-1 in myogenesis was tested using an antibody neutralization approach. ICAM-1+ cells were washed three times in phosphate buffered saline (PBS) and then treated with differentiation medium supplemented with vehicle (water), an ICAM-1 neutralizing antibody (YN1/1.7.4; eBioscience; 100 μg/ml) or an isotype control antibody (eBioscience; 100 μg/ml) for 2 or 24 h. The antibody concentration was chosen based on findings from experiments that examined the influence of varying concentrations of the ICAM-1 neutralizing antibody on myotube indices. For the myoblast adhesion assay (described below), ICAM-1+ cells were suspended in differentiation medium containing vehicle, isotype control antibody (100 μg/ml), or ICAM-1 antibody (100 μg/ml) for 2 h.

Cell Penetrating Peptides

The involvement of the cytoplasmic domain of ICAM-1 in myogenesis was tested using a cell penetrating peptide that competitively inhibits the binding of the cytoplasmic domain of ICAM-1 to downstream adaptor and signaling proteins (ICAM-1 peptide) [20–22]. This peptide consisted of amino acids of antennapedia (RQIKIWFQNRRMKWKK) followed by 13 (out of 27) amino acids of the cytoplasmic domain of murine ICAM-1 (QRKIRIYKLQKAQ). The control peptide contained the amino acid sequence for antennapedia and rat rhodopsin (CKPMSNFRFGENH), an irrelevant peptide [20–22]. Peptides were synthesized by Ohio Peptides Inc. Cultured cells were washed three times in PBS and then treated with differentiation medium supplemented with a peptide (50 or 100 μg/ml) or vehicle (water) for 2 or 24 h.

Western blotting

Cells were collected in reducing sample buffer (2% sodium dodecyl sulphate, 50mM tris(2-carboxyethyl)phosphine hydrochloride, 80 mM Tris-HCL and 10% glycerol) containing protease inhibitors (1mM EDTA, 5μg/ml leupeptin, 5μg/ml aprotinin, and 11 mM 4-(2-aminoethyl) benzenesulfonyl fluoride) and then sonicated (Misonix; Model S-4000). Samples were boiled and separated on 10% SDS-PAGE gels (25 μg of protein per lane). Proteins were transferred for 1 h to PVDF-FL membranes (Millipore) in Towbin's transfer buffer containing 10% methanol using a semi-dry (20 volts) or a wet transfer (200 mA) protocol. Membranes were blocked (Licor Odyssey® Blocking Buffer or 5% non-fat dry milk) and incubated overnight at 4°C with an antibody that recognizes ICAM-1 (R&D Systems Cat # AF796), myogenin (clone FD5; BD Pharmingen Cat# 556358), total-p38α (Santa Cruz Cat# SC-535), phospho-p38 (Thr180/Tyr182) (Cell Signaling Cat# 9211), puromycin [23], total Akt (Cell Signaling Cat # 9272), phospho-Akt (Ser473) (Cell Signaling Cat # 9271), total p70s6k (Cell Signaling Cat# 2708), phospho-p70s6k (Thr389) (Santa Cruz Cat # SC-11759), α-tubulin (Cell Signaling Technology Cat # 3873), or glyceraldehyde 3-phosphate dehydrogenase (GAPDH; Cell Signaling Cat# 2118) antibody.

Detection of antibody binding was achieved by using an Alexa Fluor® 680 secondary antibody (Invitrogen) and the Odyssey® infrared detection system.

Protein Synthesis

Protein synthesis was measured in cells treated with differentiation medium for up to 6 d using a nonradioactive western blotting technique known as surface sensing of translation [23, 24]. Cells were washed three times in PBS and treated with differentiation medium containing 1 μM puromycin (an analog of tyrosyl-tRNA) for 30 min at 37°C in a 5% CO_2 humidified environment [24]. Cells were collected and analyzed for incorporation of puromycin into nascent peptide chains via western blot analysis as described above.

Immunofluorescence

Cells were washed, fixed in 70% methanol/30% acetone, and permeabilized with 0.05% triton X-100 or 1 N HCl (BrdU labeling). For myogenin labeling, cells were fixed in 2% formaldehyde followed by 70% methanol/30% acetone. Cells were treated with blocking buffer (3% bovine serum albumin, 0.05% Tween-20, 0.2% gelatin in PBS) and then one of the following antibodies for 2 h: anti-ICAM-1 (R&D Systems product # AF796), anti-5-bromo-2′-deoxyuridine (BrdU) (Developmental Studies Hybridoma Bank), anti-myogenin (clone FD5; Developmental Studies Hybridoma Bank), anti-sarcomeric myosin heavy chain (MHC) (1:20; clone MF20; Developmental Studies Hybridoma Bank), anti-CD11a (clone M17/4; eBiosciences), or anti-CD11b (clone M1/70; BD Pharmingen). Cells were then incubated with a fluorochrome-conjugated secondary antibody (Invitrogen) and mounted with Fluoromount-G™ containing 4′,6-Diamidino-2-phenylindole (DAPI; SouthernBiotech).

For image analysis, six fields per well were visualized using a 10X objective on an epifluorescence microscope (Olympus IX70; B&B Microscopes), and captured with a CCD camera (RT KE SPOT™; Diagnostic Instruments). The first image was taken at the center of the well, and the second image was taken two fields of view (400 μm) to the right of the first image. The remaining four images were captured four fields of view (800 μm) from the preceding image, and collectively depicted a square in the center of the well. The same camera settings (i.e., exposure, gain, and gamma) were used for all images captured for a data set. The standardized approach to image capture was used to avoid investigator bias.

Myoblast Proliferation

Myoblast proliferation in growth medium was quantified by collecting cells using trypsin and counting them in a hemocytometer. Proliferation in differentiation medium was quantified by the incorporation of BrdU into nuclei. Cells were pulse labeled with BrdU (100 μM; Sigma-Aldrich) for 2 h at 1, 2, and 3 d of differentiation. Detection of BrdU and image capture was performed as described above. The number of BrdU+ nuclei was counted using image analysis software (Image Pro 7; Media Cybernetics Inc.), and was expressed as a percentage of the total number of nuclei. On average, ~5,000 nuclei per well were analyzed.

Myoblast Differentiation

The relative abundance of myogenin protein and its nuclear localization were determined via western blotting and immunofluorescence. Fluorescent images of myogenin and nuclei were captured in six standardized fields of view, and the percentage of nuclei containing myogenin was quantified using image analysis software (Image Pro 7; Media Cybernetics Inc.). On average, ~5,000 nuclei per well were analyzed.

The activity of creatine kinase was quantified as a biochemical marker for the later stage of differentiation [25]. Cells were collected in lysis buffer (1% Igepal®; Sigma-Aldrich) containing protease inhibitors. Lysates were centrifuged and supernatants were incubated with a creatine kinase assay reagent (Sigma Diagnostics). The rate of absorbance at 340 nm was measured at 30 second intervals for 3 minutes with a spectrophotometer. Creatine kinase activity (U/L) was subsequently calculated from changes in the rate of absorbance according to manufacturer's instruction, and normalized to total protein concentration (mU/mg).

Myoblast Adhesion

A cell suspension adhesion assay was performed using published procedures [26, 27]. Cells were seeded at high density (18,000 cells/cm^2) in growth medium and allowed to adhere for 2 h. Myoblasts were then treated with differentiation medium for 24 h to generate fusion competent myoblasts [26]. Cells were collected using StemPro® Accutase® (Invitrogen), centrifuged, suspended in differentiation medium (200 cells/μl), and placed in a rotary shaking water bath (37°C and 80 rpm) for 2 h. The total number of cells at the beginning of the incubation (N_0), and the number of single cells at 15, 30, 45, 60, 90, and 120 min of incubation (N_T), was counted using a hemocytometer. Percent aggregation at each interval was calculated using the following equation: $(N_0 - N_T / N_0) \times 100$. Cell viability was assessed by incubating cells with Evan's blue dye and viewing them via epifluorescence microscopy.

At 15, 60, and 120 min of incubation, 15,000 cells were added to a cytospin funnel (Thermo Scientific) using sterile pipette tips that had been cut to an opening of greater than 5 mm. Funnels were centrifuged (Cytospin 4; Thermo Scientific) and cytospin prepared slides were fixed in 2.5% glutaraldehyde, treated with 0.05% triton X100, and mounted with Fluoromount-G™ (SouthernBiotech). Images of glutaraldehyde-induced fluorescence (FITC setting) were captured in six standardized fields of view. The number of cells within an aggregate of cells was quantified using the cluster function of Image Pro 7 analysis software (Media Cybernetics Inc.).

Myotube Number and Size

Merged images of MHC and nuclei were analyzed using macro functions written for image analysis software (Image Pro 7; Media Cybernetics Inc.). Briefly, blue (DAPI) and green (FITC) colors were extracted from a merged image to create separate luminance images of nuclei and MHC, respectively. These images were then calibrated to the 10X objective. Using the luminance image of nuclei, the number of nuclei was counted using the cluster function. An outline of MHC labeling was created in the luminance image of MHC and then

merged with the luminance image of nuclei. This merged image was used to quantify dependent measures.

Differentiated myoblasts were operationally defined as MHC+ mononuclear cells with an area greater than 100 μm^2; whereas, myotubes were operationally defined as MHC+ cells with 2 or more nuclei and an area greater than 200 μm^2. Using these definitions, the software counted the number of nuclei, myotubes, and nuclei within a myotube (myonuclear number), as well as determined the length, maximum width, area, and mean diameter (average length of diameter measured at 2 degree intervals and passing through the centroid) of individual myotubes. The fusion index, which reflects myotube formation and myonuclei accretion, was calculated by expressing the number of nuclei within myotubes as a percentage of total nuclei. On average, ~8,000 nuclei per well were analyzed. In the later days of treatment with differentiation medium myotubes often extend outside a field of view. In this situation, measurements were made for the portion of the myotube that was in the field of view. We did not exclude myotubes that extend outside the field of view from our analysis as this would have substantially reduced the total number of myotubes in which quantitative measurements were made, and bias our data to short myotubes.

Myotube Alignment

The alignment of myotubes was quantified through two dimensional FFT analysis using a macro function created by Media Cybernetics using published procedures [28, 29]. Briefly, the software decomposed a luminance image of MHC expression into its sine and cosine components and then converted the spatial information into a mathematically defined frequency domain. Pixel intensities were summed for each angle (0–360°), normalized to the lowest intensity value, and plotted against angle to produce a FFT alignment plot [28]. The degree of alignment is indicated by peak normalized sum intensity and the overall shape of the FFT alignment plot [28]. The shape of the alignment plot was quantified by calculating the area under the curve using the trapezoid rule method.

Statistical Analyses

Using Sigma Stat statistical software (Systat), data sets were analyzed using one or two way analysis of variance (ANOVA). The Newman-Keuls *post-hoc* test was then used to locate the differences between groups when the observed F ratio was statistically significant ($p<0.05$). Data are reported as mean and standard error. The reported sample size for a given dependent measure represents the number of replicates per group in 3 or more separate experiments.

Results

ICAM-1 Expression

As skeletal muscle cells do not constitutively express ICAM-1 [10, 16, 17], we used a stable transfection approach to reveal the extent to which ICAM-1 expression by skeletal muscle cells influences myogenesis. Flow cytometry revealed that greater than 90% of the myoblasts transfected with the ICAM-1 plasmid expressed ICAM-1 (ICAM-1+; Fig. S1A). As expected, western blotting failed to detect ICAM-1 in cultures containing either control

or empty vector (EV) myoblasts (Fig. S1B). In contrast, ICAM-1+ cells expressed high levels of ICAM-1. The ICAM-1 band observed for ICAM-1+ cells was of the same molecular weight as that found for control myoblasts treated with TNF-α (10 ng/ml of rmTNF-α for 24 h), a treatment that caused 30% of the myoblasts to express ICAM-1 [10]. In ICAM-1+ cells, ICAM-1 expression remained high throughout 6 d of differentiation in both myotubes and non-fused myoblasts (Fig. S1C and D). Collectively, our findings demonstrate the creation of a murine skeletal muscle cell line that expresses ICAM-1.

ICAM-1 Expression does not Influence Myoblast Proliferation

We first determined if ICAM-1 expression by myoblasts influences their ability to proliferate. Myoblast number was similar between the cell lines at 2–4 d of treatment with growth medium (Fig. S1E). Proliferation in differentiation medium was assessed by quantifying the incorporation of BrdU into nuclei (Fig. S1F). The percentage of BrdU+ nuclei at 1–3 d of differentiation was similar between the cell lines (Fig. S1G). These data demonstrate that ICAM-1 expression by myoblasts does not influence their proliferation in growth or differentiation medium.

ICAM-1 Expression does not Influence Myoblast Differentiation

The influence of ICAM-1 expression on myoblast differentiation was assessed by quantifying the expression and nuclear localization of myogenin, and the activity of creatine kinase. The relative abundance of myogenin protein, percentage of nuclei expressing myogenin, and creatine kinase activity were similar between the cell lines through 3 d of differentiation (Fig. 1A–E). As p38 MAPK signaling facilitates myoblast differentiation [6, 30, 31], phosphorylated levels of p38 MAPK were used as readout of the extent to which ICAM-1 expression influences cell signaling for myoblast differentiation. Phosphorylated (Thr180/Tyr182) and total p38α MAPK were similar between the cell lines throughout 3 d differentiation (Fig. 1F and G). Lastly, treatment of ICAM-1+ cells at 1 d of differentiation for 2 or 24 h with a cell penetrating peptide that blocks the signal transducing function of the cytoplasmic domain of ICAM-1 [20–22], failed to influence myogenin expression and phosphorylated levels of p38 MAPK (Fig. S2). Collectively, these data demonstrate that the expression of ICAM-1 by myoblasts does not influence their ability to differentiate.

ICAM-1 Expression Augments Nascent Myotube Formation and Myonuclear Number

The extent to which ICAM-1 expression influences myotube formation and myonuclei accretion was determined through quantitative analysis of myosin heavy chain (MHC) and nuclei staining (Fig. 2A). The number of myotubes was 2 fold higher at 2 and 3 d of differentiation in ICAM-1+ compared to control and empty vector cells (Fig. 2B). Furthermore, myonuclear number and percentage of nuclei within myotubes (i.e., fusion index) were 2–3 fold higher in ICAM-1+ compared to control and empty vector cells at 2 and 3 d of differentiation (Fig. 2C and D). These data demonstrate that ICAM-1 expression enhances nascent myotube formation and subsequent myonuclear accretion.

ICAM-1 Expression Augments Myotube-Myotube Fusion and Myotube Size

ICAM-1 expression influenced myotube number after nascent myotube formation reached a plateau (i.e., after 3 d of differentiation). In ICAM-1+ cells, the number of myotubes at 5 and 6 d of differentiation was ~2 fold lower compared to control and empty vector cells (Fig. 2B). In contrast, myonuclei number and fusion index were 2–4 fold higher at 5 and 6 d of differentiation for ICAM-1+ compared to control and empty vector cells (Fig. 2C). These findings of a reduced number of myotubes and a concomitant increase in myonuclei number indicate that ICAM-1 expression augmented fusion of mature myotubes.

The average length, diameter, area (Fig. 2E–G), as well as maximum width (data not reported) of myotubes were 1.3–3 fold higher in ICAM-1+ compared to control and empty vector cells at 3–6 d of differentiation. These data demonstrate that ICAM-1 expression augmented myotube hypertrophy.

ICAM-1 Expression Enhances Myoblast Adhesion

As myotube formation and myonuclear accretion is dependent on myoblast adhesion [2, 3], we examined the influence of ICAM-1 expression on myoblast adhesion in a 2 h cell suspension assay. Percent aggregation was 3 and 1.7 fold higher in ICAM-1+ compared to control and empty vector cells at 15–30 and 45–120 min of the assay, respectively. The average number of cells in aggregates was similar between the cell lines at 15 min, and 2.5 fold higher for ICAM-1+ cells was compared to control and empty vector cells at 60 and 120 min of the assay (Fig. 3B and C). These data indicate that ICAM-1 expression facilitated myoblast-myoblast adhesion by initially increasing the rate of aggregate formation, and subsequently by increasing the number of cells in aggregates. These findings demonstrate that ICAM-1 expression augments homotypic adhesion of fusion competent myoblasts.

ICAM-1 Expression Facilitates Myotube Alignment

Nascent myotubes *in vitro* initially adopt a random pattern of alignment and align themselves just prior to myotube-myotube fusion [32–34]. To explore mechanisms through which ICAM-1 expression augments myotube fusion, and the resulting increase in myonuclear number and myotube size, we quantified the degree of alignment of myotubes using fast Fourier transform (FFT) analysis [28, 29]. This analysis converted the spatial information within an image of MHC and nuclei staining (Fig. 4A) into a mathematically defined frequency domain, resulting in a FFT plot with low frequency pixels at the origin and high frequency pixels away from the origin (Fig. 4B). Pixel intensities are plotted against angle (0–360°) to produce a FFT alignment plot (Fig. 4C). Peak normalized sum intensity and the overall shape of the FFT alignment plot reflect the degree of alignment [28].

As expected, control and empty vector myotubes showed more than one axis of alignment as indicated by a broad pattern in FFT alignment plots and low peak sum intensities (Fig. 4A–C). In contrast, ICAM-1+ myotubes showed a high degree of alignment. Peak sum intensities and areas under the curve (a measure of the overall shape of the FFT alignment plot) were 50–60% higher at 2–6 d of differentiation for ICAM-1+ compared to control and

empty vector cells (Fig. 4D and E). These data demonstrate that ICAM-1 expression induced the parallel alignment of nascent and mature myotubes.

Extracellular and Cytoplasmic Domains of ICAM-1 Regulates Early Events of Myogenesis

To substantiate the involvement of ICAM-1 in the regulation of the early events of myogenesis, we inhibited the adhesive and signaling function of ICAM-1 by treating cells with a neutralizing antibody or peptide, respectively at 1 d of differentiation. Antibody blockade of the extracellular domain of ICAM-1 reduced the number of cells within aggregates (Fig. 5A). In contrast, percent aggregation was not reduced by antibody neutralization of ICAM-1 (Fig. 5B). This finding was most likely attributable to an insufficient amount of time for antibody neutralization of ICAM-1 prior to the formation of aggregates, as 45% of the vehicle treated cells formed aggregates within 15 min of incubation. Importantly, myotube formation, myonuclear number, fusion index, myotube alignment (Fig. 5C–G), as well as indices of myotube size (data not reported) were reduced by treatment with ICAM-1 antibody. Peptide inhibition of the cytoplasmic domain of ICAM-1 also reduced myotube formation, myonuclear number, fusion index, myotube alignment (Fig. 5H–L), as well as indices of myotube size (data not reported). As expected, treatment of control and EV cells with ICAM-1 antibody or peptide did not reduce myotube indices (data not reported). Collectively, these data indicate that adhesion-induced activation of ICAM-1 signaling in skeletal muscle cells augments myotube formation, myonuclear accretion, and myotube alignment.

Extracellular and Cytoplasmic Domains of ICAM-1 Regulates Later Events of Myogenesis

To substantiate the involvement of ICAM-1 in myotube fusion and hypertrophy, we treated ICAM-1+ cells with ICAM-1 antibody or peptide at 5 d of differentiation. Both antibody (Fig. 6A–D) and peptide (Fig. 7A–D) inhibition of ICAM-1 increased myotube number, as well as decreased myonuclei number and fusion index. The ICAM-1 antibody and peptide also reduced alignment, diameter, and area of myotubes (Fig. 6E–G and Fig. 7E–G), as well as myotube length and width (data not reported). Collectively, these data indicate that adhesion-induced activation of ICAM-1 signaling in skeletal muscle cells augments myotube hypertrophy by facilitating myotube fusion.

As sustained elevations in protein synthesis induce skeletal muscle cell hypertrophy [24, 35], we quantified the extent to which ICAM-1 expression influences protein synthesis using a nonradioactive western blotting technique [23, 24]. Protein synthesis was 3 fold higher in ICAM-1+ compared to control and empty vector cells throughout 6 d of differentiation (Fig. 8A). Total protein was 25% higher in ICAM-1+ compared to control and empty vector cells throughout 6 d of differentiation (data not reported; n=6). To establish the involvement of the extracellular and cytoplasmic domains of ICAM-1 in protein synthesis, we treated cells with the ICAM-1 antibody or peptide at 5 d of differentiation for 2 h. The ICAM-1 antibody reduced protein synthesis in ICAM-1+ cells by 76% compared to cells treated with vehicle and isotype control antibody (data not reported; n=4). Importantly, peptide inhibition of ICAM-1 (Fig. 8B) reduced protein synthesis to levels that were observed in control and empty vector cells. As expected, ICAM-1 peptide did not influence protein synthesis in

control and empty vector cells. These data indicate that the adhesive and signaling functions of ICAM-1 augmented myotube hypertrophy by elevating protein synthesis.

As protein synthesis in skeletal muscle cells is regulated by Akt and mTOR [7, 35], we analyzed levels of Akt and p70s6k (a downstream target of mTOR) in control, empty vector, and ICAM-1+ cells through 6 d of differentiation, as well as in ICAM-1+ cells treated with ICAM-1 peptide at 5 d of differentiation. Phosphorylated, but not total, levels of Akt (Ser473) and p70s6k (Thr389) were 2 fold higher in ICAM-1+ compared to control and empty vector cells at 3–6 d of differentiation (Fig. 8C). Compared to vehicle and control peptide, ICAM-1 peptide reduced phosphorylated, but not total, levels of Akt and p70s6k in ICAM-1+ cells (Fig 8D). These findings demonstrate that the signal transducing function of ICAM-1 augmented protein synthesis via a mechanism involving Akt and p70s6k signaling.

Skeletal Muscle Cells do not Express CD11a or CD11b

We explored skeletal muscle cell expression of CD11a and CD11b to gain insight into the possibility that their interaction with ICAM-1 served as a mechanism for initiating ICAM-1 signaling. Although CD11a and CD11b were found to be expressed in peritoneal leukocytes (positive control), we did not detect their expression in skeletal muscle cells (control, empty vector, and ICAM-1+) treated with differentiation medium for up to 6 d (Fig. S3). Western blotting and immunoprecipitation for CD11a and CD11b were not performed on lysates of skeletal muscle cells, as both approaches failed to detect a band at their anticipated molecular weight (160–180 kDa) in peritoneal leukocytes using established antibodies. Nevertheless, our immunofluorescence findings are in agreement with prior work that demonstrated that cultured myoblasts and myotubes do not express β2 integrins [9, 16, 17, 36].

ICAM-1 mediated Myogenesis is not dependent on Serum

We explored the possibility that fibrinogen, which binds to ICAM-1 [37], or other serum components served as a mechanism for initiating ICAM-1 signaling by treating ICAM-1+ cells with serum free medium containing insulin, transferrin, and selenium (ITS). In ITS medium, myotube number, average number of nuclei within myotubes, fusion index, and measures of myotube size were similar to values observed for serum containing differentiation medium (Fig. S4A–F). These findings demonstrate that phenotypic alterations resulting from the expression of ICAM-1 were not dependent on the presence of horse serum in differentiation medium.

Discussion

ICAM-1 is a member of the immunoglobulin superfamily of adhesion molecules [14, 15] that is not constitutively expressed by skeletal muscle cells [10, 16, 17]. We recently reported that muscle overload induced the expression of ICAM-1 by skeletal muscle cells, which contributed to the ensuing regenerating myofiber formation, as well as myofiber and whole muscle hypertrophy [10]. The present study utilized an *in vitro*, stable transfection approach to determine the extent to which ICAM-1 expression by skeletal muscle cells facilitates myogenic processes pertinent to muscle regeneration and hypertrophy. We found

that the expression of ICAM-1 by skeletal muscle cells augmented myoblast adhesion and subsequent fusion to myoblasts and myotubes, as well as myotube alignment, fusion, and size without influencing the ability of myoblasts to proliferate or differentiate. ICAM-1 augmented events of myogenesis through mechanisms involving its adhesive and signaling functions. Taken together, our *in vivo* and *in vitro* findings support a novel paradigm in which the expression of ICAM-1 by skeletal muscle cells facilitates growth processes in skeletal muscle.

A major finding of the present study was that ICAM-1 expression by myoblasts increased nascent myotube formation and their subsequent myonuclear accretion by augmenting homotypic adhesion of myoblasts. These findings are consistent with our *in vivo* observations after muscle overload. Specifically, muscle overload induced the expression of ICAM-1 by satellite cells/myoblasts, and regenerating myofiber formation was substantially impaired in overloaded ICAM-1−/− mice [10]. As satellite cells/myoblasts are required for the development of regenerating myofibers in overloaded and injured muscles [11, 38], our *in vitro* findings indicate that the expression of ICAM-1 by satellite cells/myoblasts *in vivo* facilitates regenerating myofiber formation by increasing adhesion and subsequent fusion of myoblasts.

Other members of the immunoglobulin superfamily of adhesion molecules, such as neural cell adhesion molecule (NCAM; CD56) and vascular cell adhesion molecule-1 (VCAM-1; CD106) have been reported to facilitate myoblast adhesion and/or fusion [2, 3]. In contrast to ICAM-1, NCAM and VCAM-1 are constitutively expressed by cultured myoblasts and myotubes [39, 40]. Although the contribution of NCAM and VCAM-1 to *in vivo* myogenesis is controversial [2, 3], antibody neutralization of NCAM and VCAM-1 *in vitro* has been reported to reduce myoblast-myoblast adhesion and/or the percentage of nuclei within myotubes (i.e., fusion index) [27, 39]. NCAM facilitates cell-to-cell adhesion through the homophilic interaction of NCAM on opposing membranes [41] and regulates myoblast fusion through glycosylation of the extracellular domain [42]. The expression of VCAM-1 by myoblasts has been suggested to facilitate their fusion by binding to VLA-4 (α4 integrin; CD49d) expressed by myoblasts and myotubes [39]. Homophilic binding and glycosylation could serve as mechanisms for ICAM-1 mediated myoblast adhesion and fusion as ICAM-1 shares sequence homology with NCAM [43], forms dimers or multimers on plasma membranes [44, 45], and contains multiple glycosylation sites [46]. Although binding of CD11a or CD11b to ICAM-1 promotes cell-to-cell adhesion [14, 15] and macrophage-macrophage fusion [47], β2 integrin-ICAM-1 interactions did contribute to ICAM-1 mediated myoblast adhesion and fusion as cultured skeletal muscle cells do not express β2 integrins [present study, 9, 16, 17, 36]. In addition to facilitating cell-to-cell interactions, ICAM-1 expression by myoblasts could enhance their adhesion to the extracellular matrix, as ICAM-1 has been reported to bind to hyaluronan [48], a polysaccharide of the extracellular matrix that appears to be expressed by cultured myoblast and myotubes [49]. Thus, ICAM-1 expression could enhance adhesion and subsequent fusion of myoblasts through multiple mechanisms involving the adhesive function of the extracellular domain of ICAM-1.

Prior investigators have demonstrated in endothelial cells that ligation of the extracellular domain of ICAM-1 activates intracellular signaling pathways (e.g., p38 MAPK, Akt, Rho GTPases) through the association of the cytoplasmic domain of ICAM-1 with adaptor and other cytoskeletal proteins [14, 15]. In ICAM-1+ cells, inhibition of the extracellular and cytoplasmic domains of ICAM-1 reduced nascent myotube formation and myonuclear accretion. These results indicate that ICAM-1 mediated myoblast adhesion regulates their subsequent fusion to myoblasts and myotubes by initiating ICAM-1 signaling. Several signaling pathways regulate myoblast fusion by facilitating myoblast differentiation (e.g., p38 MAPK and Akt) [6, 30, 31, 50]; whereas, other pathways (e.g., Rac1 GTPase and ERK5) augment myoblast fusion through a mechanism that is independent from myoblast differentiation [51–53]. As ICAM-1 expression did not influence myoblast differentiation or phosphorylated levels of p38 MAPK and Akt (1–2 d of differentiation; data not reported), we speculate that ICAM-1 augmented myoblast fusion by increasing Rac1 and/or ERK5 signaling.

Myotubes *in vitro* adopt a random pattern of alignment, which is in contrast to the high degree of alignment of myofibers in whole muscles. Prior researchers using time lapse microscopy have made qualitative observations of myotube migration, alignment, and fusion [32–34]. However, no studies to our knowledge have quantified myotube alignment or determined its contribution to myotube-myotube fusion. Strikingly, ICAM-1 expression increased the parallel alignment of myotubes (nascent and mature) and facilitated fusion of mature myotubes, resulting in an increase in myonuclei number.

An increase in myonuclear number is thought to serve as a mechanism for myotube and myofiber hypertrophy by increasing their capacity for protein synthesis. In the present study, ICAM-1 mediated myotube hypertrophy was accompanied by an increased number of myonuclei and a greater rate of protein synthesis. The hypertrophic phenotype of ICAM-1+ myotubes closely parallels our *in vivo* findings after muscle overload [10]. Specifically, ICAM-1+ myofibers in overloaded muscles were larger than myofibers that did not express ICAM-1, and protein synthesis and measures of hypertrophy (e.g., total protein and myofiber size) were attenuated in overloaded ICAM-1−/− compared to wild type mice [10]. Myotube and myofiber hypertrophy, particularly after mechanical loading or treatment with insulin or insulin-like growth factor-1, occur through mechanisms involving myonuclear accretion, increased protein synthesis, and the activity of Akt and/or mTOR [7, 8, 54, 55]. These mechanisms contributed to the hypertrophic phenotype of ICAM-1+ cells as inhibition of ICAM-1 reduced myonuclei number, protein synthesis, phosphorylated levels of Akt and p70s6k, as well as myotube size. Taken together, our *in vivo* and *in vitro* findings demonstrate that the expression of ICAM-1 by differentiated skeletal muscle cells facilitates their hypertrophy.

In our prior *in vivo* work [10], we speculated that interactions between β2 integrins expressed by myeloid cells and ICAM-1 expressed by myofibers facilitate protein synthesis and myofiber hypertrophy after muscle overload through the release of cytokines from myeloid cells. The results from the present study do not negate this potential mechanism; rather the data supports an alternative, cell intrinsic mechanism through which ICAM-1 expression by myofibers could facilitate their hypertrophy after muscle overload.

Specifically, ICAM-1 expression by myofibers *in vivo* could increase protein synthesis and myofiber size through a mechanism that is not dependent on ligation by β2 integrins. Clearly, further study is needed to reveal the specific contribution of ICAM-1 expression by skeletal muscle cells to regenerative and hypertrophic processes *in vivo*.

Conclusions

In summary, the expression of ICAM-1 by cultured skeletal muscle cells augmented events of myogenesis in which myotubes are forming, adding nuclei, aligning, fusing, synthesizing proteins, and hypertrophying, without influencing their ability to proliferate or differentiate. ICAM-1 augmented myotube formation and myonuclear accretion by increasing cell-to-cell adhesion; whereas, ICAM-1 augmented myotube size by enhancing myotube alignment, myotube-myotube fusion, protein synthesis, and Akt/p70s6k signaling. These novel findings contribute to a growing body of literature that supports a role of adhesion molecules of the inflammatory response in the regulation of growth processes in skeletal muscle [9, 10, 13]. Future studies will need to reveal the function of ICAM-1 expressed by primary skeletal muscle cells, as well as how ICAM-1 signaling in skeletal muscle cells is initiated and controlled, before the role of ICAM-1 in myogenesis is established. Results from these studies will help define novel therapeutic targets that restore structure and function to injured muscles, and facilitate the maintenance and/or growth of skeletal muscle, particularly in older individuals.

Supplementary Material

Refer to Web version on PubMed Central for supplementary material.

Acknowledgments

This research was supported by grants from the American College of Sports Medicine Doctoral Student Research Program (QG and CLD), the University of Toledo Interdisciplinary Research Initiation Program (DNC and FXP), and National Institute of Health (R15AR064858; FXP). The authors acknowledge Douglas Leaman for his assistance in creating the cell lines, as well as the technical support staff at B&B Microscopes Inc. and Media Cybernetics Inc. for their assistance in image analysis.

References

1. Yin H, Price F, Rudnicki MA. Satellite cells and the muscle stem cell niche. Physiological reviews. 2013; 93:23–67. [PubMed: 23303905]
2. Pavlath, GK. Current Progress Towards Understanding Mechanisms of Myoblast Fusion in Mammals. Springer-Verlag; Berlin, Heidelberger Platz 3, D–14197 Berlin, Germany: 2011.
3. Krauss RS. Regulation of promyogenic signal transduction by cell-cell contact and adhesion. Experimental cell research. 2010; 316:3042–3049. [PubMed: 20471976]
4. Hindi SM, Tajrishi MM, Kumar A. Signaling mechanisms in Mammalian myoblast fusion. Science signaling. 2013; 6:re2. [PubMed: 23612709]
5. Abmayr SM, Pavlath GK. Myoblast fusion: lessons from flies and mice. Development. 2012; 139:641–656. [PubMed: 22274696]
6. Knight JD, Kothary R. The myogenic kinome: protein kinases critical to mammalian skeletal myogenesis. Skelet Muscle. 2011; 1:29. [PubMed: 21902831]
7. Schiaffino S, Mammucari C. Regulation of skeletal muscle growth by the IGF1-Akt/PKB pathway: insights from genetic models. Skelet Muscle. 2011; 1:4. [PubMed: 21798082]

8. Goodman CA, Frey JW, Mabrey DM, Jacobs BL, Lincoln HC, You JS, Hornberger TA. The role of skeletal muscle mTOR in the regulation of mechanical load-induced growth. The Journal of physiology. 2011; 589:5485–5501. [PubMed: 21946849]
9. Marino JS, Tausch BJ, Dearth CL, Manacci MV, McLoughlin TJ, Rakyta SJ, Linsenmayer MP, Pizza FX. Beta2-integrins contribute to skeletal muscle hypertrophy in mice. American journal of physiology. Cell physiology. 2008; 295:C1026–1036. [PubMed: 18753316]
10. Dearth CL, Goh Q, Marino JS, Cicinelli PA, Torres-Palsa MJ, Pierre P, Worth RG, Pizza FX. Skeletal muscle cells express icam-1 after muscle overload and icam-1 contributes to the ensuing hypertrophic response. PLoS One. 2013; 8:e58486. [PubMed: 23505517]
11. McCarthy JJ, Mula J, Miyazaki M, Erfani R, Garrison K, Farooqui AB, Srikuea R, Lawson BA, Grimes B, Keller C, Van Zant G, Campbell KS, Esser KA, Dupont-Versteegden EE, Peterson CA. Effective fiber hypertrophy in satellite cell-depleted skeletal muscle. Development. 2011; 138:3657–3666. [PubMed: 21828094]
12. Guerci A, Lahoute C, Hebrard S, Collard L, Graindorge D, Favier M, Cagnard N, Batonnet-Pichon S, Precigout G, Garcia L, Tuil D, Daegelen D, Sotiropoulos A. Srf-dependent paracrine signals produced by myofibers control satellite cell-mediated skeletal muscle hypertrophy. Cell metabolism. 2012; 15:25–37. [PubMed: 22225874]
13. Pizza FX, Peterson JM, Baas JH, Koh TJ. Neutrophils contribute to muscle injury and impair its resolution after lengthening contractions in mice. J Physiol. 2005; 562:899–913. [PubMed: 15550464]
14. van de Stolpe A, van der Saag PT. Intercellular adhesion molecule-1. J Mol Med. 1996; 74:13–33. [PubMed: 8834767]
15. Lawson C, Wolf S. ICAM-1 signaling in endothelial cells. Pharmacol Rep. 2009; 61:22–32. [PubMed: 19307690]
16. Goebels N, Michaelis D, Wekerle H, Hohlfeld R. Human myoblasts as antigen-presenting cells. J Immunol. 1992; 149:661–667. [PubMed: 1352532]
17. Michaelis D, Goebels N, Hohlfeld R. Constitutive and cytokine-induced expression of human leukocyte antigens and cell adhesion molecules by human myotubes. Am J Pathol. 1993; 143:1142–1149. [PubMed: 8214008]
18. Siu G, Hedrick SM, Brian AA. Isolation of the murine intercellular adhesion molecule 1 (ICAM-1) gene. ICAM-1 enhances antigen-specific T cell activation. J Immunol. 1989; 143:3813–3820. [PubMed: 2479693]
19. Gunning P, Leavitt J, Muscat G, Ng SY, Kedes L. A human beta-actin expression vector system directs high-level accumulation of antisense transcripts. Proc Natl Acad Sci U S A. 1987; 84:4831–4835. [PubMed: 2440031]
20. Greenwood J, Amos CL, Walters CE, Couraud PO, Lyck R, Engelhardt B, Adamson P. Intracellular domain of brain endothelial intercellular adhesion molecule-1 is essential for T lymphocyte-mediated signaling and migration. J Immunol. 2003; 171:2099–2108. [PubMed: 12902516]
21. Oh HM, Lee S, Na BR, Wee H, Kim SH, Choi SC, Lee KM, Jun CD. RKIKK motif in the intracellular domain is critical for spatial and dynamic organization of ICAM-1: functional implication for the leukocyte adhesion and transmigration. Mol Biol Cell. 2007; 18:2322–2335. [PubMed: 17429072]
22. Sumagin R, Sarelius IH. Intercellular adhesion molecule-1 enrichment near tricellular endothelial junctions is preferentially associated with leukocyte transmigration and signals for reorganization of these junctions to accommodate leukocyte passage. J Immunol. 2010; 184:5242–5252. [PubMed: 20363969]
23. Schmidt EK, Clavarino G, Ceppi M, Pierre P. SUnSET, a nonradioactive method to monitor protein synthesis. Nat Methods. 2009; 6:275–277. [PubMed: 19305406]
24. Goodman CA, Mabrey DM, Frey JW, Miu MH, Schmidt EK, Pierre P, Hornberger TA. Novel insights into the regulation of skeletal muscle protein synthesis as revealed by a new nonradioactive in vivo technique. Faseb J. 2011; 25:1028–1039. [PubMed: 21148113]
25. Morris GE. The use of creatine kinase activity as an index of skeletal-muscle differentiation. Biochem Soc Trans. 1978; 6:509–511. [PubMed: 669001]

26. Griffin CA, Kafadar KA, Pavlath GK. MOR23 promotes muscle regeneration and regulates cell adhesion and migration. Dev Cell. 2009; 17:649–661. [PubMed: 19922870]
27. Knudsen KA, McElwee SA, Myers L. A role for the neural cell adhesion molecule, NCAM, in myoblast interaction during myogenesis. Developmental biology. 1990; 138:159–168. [PubMed: 2407576]
28. Ayres CE, Jha BS, Meredith H, Bowman JR, Bowlin GL, Henderson SC, Simpson DG. Measuring fiber alignment in electrospun scaffolds: a user's guide to the 2D fast Fourier transform approach. Journal of biomaterials science. Polymer edition. 2008; 19:603–621. [PubMed: 18419940]
29. Bajaj P, Reddy B Jr, Millet L, Wei C, Zorlutuna P, Bao G, Bashir R. Patterning the differentiation of C2C12 skeletal myoblasts. Integr Biol (Camb). 2011; 3:897–909. [PubMed: 21842084]
30. Wang H, Xu Q, Xiao F, Jiang Y, Wu Z. Involvement of the p38 mitogen-activated protein kinase alpha, beta, and gamma isoforms in myogenic differentiation. Molecular biology of the cell. 2008; 19:1519–1528. [PubMed: 18256287]
31. Perdiguero E, Ruiz-Bonilla V, Serrano AL, Munoz-Canoves P. Genetic deficiency of p38alpha reveals its critical role in myoblast cell cycle exit: the p38alpha-JNK connection. Cell Cycle. 2007; 6:1298–1303. [PubMed: 17534150]
32. Millay DP, O'Rourke JR, Sutherland LB, Bezprozvannaya S, Shelton JM, Bassel-Duby R, Olson EN. Myomaker is a membrane activator of myoblast fusion and muscle formation. Nature. 2013; 499:301–305. [PubMed: 23868259]
33. Musa H, Orton C, Morrison EE, Peckham M. Microtubule assembly in cultured myoblasts and myotubes following nocodazole induced microtubule depolymerisation. J Muscle Res Cell Motil. 2003; 24:301–308. [PubMed: 14620743]
34. Nowak SJ, Nahirney PC, Hadjantonakis AK, Baylies MK. Nap1-mediated actin remodeling is essential for mammalian myoblast fusion. Journal of cell science. 2009; 122:3282–3293. [PubMed: 19706686]
35. Goodman CA, Mayhew DL, Hornberger TA. Recent progress toward understanding the molecular mechanisms that regulate skeletal muscle mass. Cellular signalling. 2011; 23:1896–1906. [PubMed: 21821120]
36. De Rossi M, Bernasconi P, Baggi F, de Waal Malefyt R, Mantegazza R. Cytokines and chemokines are both expressed by human myoblasts: possible relevance for the immune pathogenesis of muscle inflammation. Int Immunol. 2000; 12:1329–1335. [PubMed: 10967028]
37. Languino LR, Plescia J, Duperray A, Brian AA, Plow EF, Geltosky JE, Altieri DC. Fibrinogen mediates leukocyte adhesion to vascular endothelium through an ICAM-1-dependent pathway. Cell. 1993; 73:1423–1434. [PubMed: 8100742]
38. Lepper C, Partridge TA, Fan CM. An absolute requirement for Pax7-positive satellite cells in acute injury-induced skeletal muscle regeneration. Development. 2011; 138:3639–3646. [PubMed: 21828092]
39. Rosen GD, Sanes JR, LaChance R, Cunningham JM, Roman J, Dean DC. Roles for the integrin VLA-4 and its counter receptor VCAM-1 in myogenesis. Cell. 1992; 69:1107–1119. [PubMed: 1377605]
40. Moore SE, Thompson J, Kirkness V, Dickson JG, Walsh FS. Skeletal muscle neural cell adhesion molecule (N-CAM): changes in protein and mRNA species during myogenesis of muscle cell lines. J Cell Biol. 1987; 105:1377–1386. [PubMed: 3654757]
41. Rao Y, Wu XF, Gariepy J, Rutishauser U, Siu CH. Identification of a peptide sequence involved in homophilic binding in the neural cell adhesion molecule NCAM. The Journal of cell biology. 1992; 118:937–949. [PubMed: 1380002]
42. Suzuki M, Angata K, Nakayama J, Fukuda M. Polysialic acid and mucin type o-glycans on the neural cell adhesion molecule differentially regulate myoblast fusion. The Journal of biological chemistry. 2003; 278:49459–49468. [PubMed: 13679364]
43. Simmons D, Makgoba MW, Seed B. ICAM, an adhesion ligand of LFA-1, is homologous to the neural cell adhesion molecule NCAM. Nature. 1988; 331:624–627. [PubMed: 3340213]
44. Miller J, Knorr R, Ferrone M, Houdei R, Carron CP, Dustin ML. Intercellular adhesion molecule-1 dimerization and its consequences for adhesion mediated by lymphocyte function associated-1. J Exp Med. 1995; 182:1231–1241. [PubMed: 7595194]

45. Reilly PL, Woska JR Jr, Jeanfavre DD, McNally E, Rothlein R, Bormann BJ. The native structure of intercellular adhesion molecule-1 (ICAM-1) is a dimer. Correlation with binding to LFA-1. J Immunol. 1995; 155:529–532. [PubMed: 7608533]
46. Otto VI, Damoc E, Cueni LN, Schurpf T, Frei R, Ali S, Callewaert N, Moise A, Leary JA, Folkers G, Przybylski M. N-glycan structures and N-glycosylation sites of mouse soluble intercellular adhesion molecule-1 revealed by MALDI-TOF and FTICR mass spectrometry. Glycobiology. 2006; 16:1033–1044. [PubMed: 16877748]
47. Fais S, Burgio VL, Silvestri M, Capobianchi MR, Pacchiarotti A, Pallone F. Multinucleated giant cells generation induced by interferon-gamma. Changes in the expression and distribution of the intercellular adhesion molecule-1 during macrophages fusion and multinucleated giant cell formation. Laboratory investigation; a journal of technical methods and pathology. 1994; 71:737–744.
48. McCourt PA, Ek B, Forsberg N, Gustafson S. Intercellular adhesion molecule-1 is a cell surface receptor for hyaluronan. The Journal of biological chemistry. 1994; 269:30081–30084. [PubMed: 7527024]
49. Hunt LC, Gorman C, Kintakas C, McCulloch DR, Mackie EJ, White JD. Hyaluronan synthesis and myogenesis: a requirement for hyaluronan synthesis during myogenic differentiation independent of pericellular matrix formation. The Journal of biological chemistry. 2013; 288:13006–13021. [PubMed: 23493399]
50. Gardner S, Anguiano M, Rotwein P. Defining Akt actions in muscle differentiation. American journal of physiology. Cell physiology. 2012; 303:C1292–1300. [PubMed: 23076793]
51. Vasyutina E, Martarelli B, Brakebusch C, Wende H, Birchmeier C. The small G-proteins Rac1 and Cdc42 are essential for myoblast fusion in the mouse. Proceedings of the National Academy of Sciences of the United States of America. 2009; 106:8935–8940. [PubMed: 19443691]
52. Charrasse S, Comunale F, Fortier M, Portales-Casamar E, Debant A, Gauthier-Rouviere C. M-cadherin activates Rac1 GTPase through the Rho-GEF trio during myoblast fusion. Molecular biology of the cell. 2007; 18:1734–1743. [PubMed: 17332503]
53. Sunadome K, Yamamoto T, Ebisuya M, Kondoh K, Sehara-Fujisawa A, Nishida E. ERK5 regulates muscle cell fusion through Klf transcription factors. Dev Cell. 2011; 20:192–205. [PubMed: 21316587]
54. Bruusgaard JC, Johansen IB, Egner IM, Rana ZA, Gundersen K. Myonuclei acquired by overload exercise precede hypertrophy and are not lost on detraining. Proceedings of the National Academy of Sciences of the United States of America. 2010; 107:15111–15116. [PubMed: 20713720]
55. Rommel C, Bodine SC, Clarke BA, Rossman R, Nunez L, Stitt TN, Yancopoulos GD, Glass DJ. Mediation of IGF-1-induced skeletal myotube hypertrophy by PI(3)K/Akt/mTOR and PI(3)K/Akt/GSK3 pathways. Nat Cell Biol. 2001; 3:1009–1013. [PubMed: 11715022]

Highlights

- We examined mechanisms through which skeletal muscle cell expression of ICAM-1 facilitates events of *in vitro* myogenesis.
- Expression of ICAM-1 by cultured myoblasts did not influence their ability to proliferate or differentiate.
- Skeletal muscle cell of ICAM-1 augmented myoblast fusion, myotube alignment, myotube-myotube fusion, and myotube size.
- ICAM-1 augmented myogenic processes through mechanisms involving its adhesive and signaling functions.

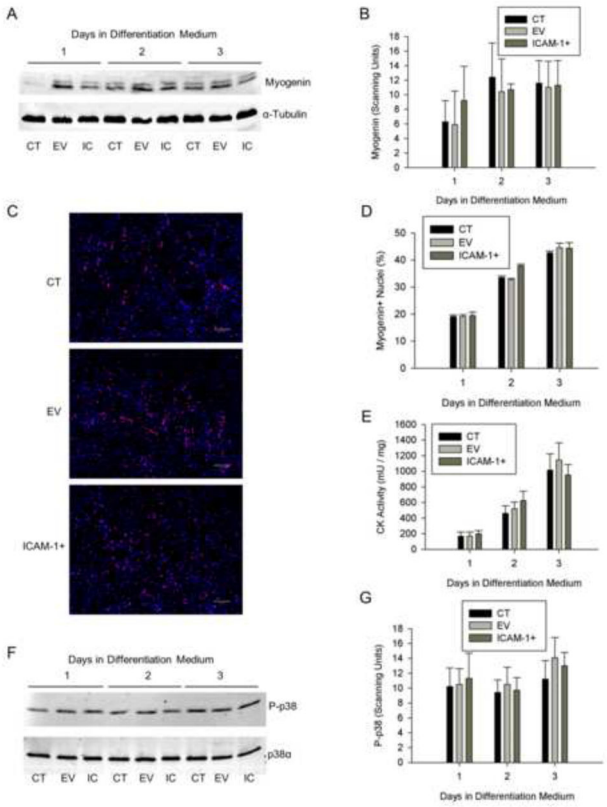

Figure 1.

Myoblast differentiation. A) Representative western blot of myogenin (25 kDa) and α-tubulin (50 kDa; loading control) in control (CT), empty vector (EV), and ICAM-1+ (IC) cells through 3 d of differentiation. B) Quantitative analysis of western blot detection of myogenin (n=4). C) Representative images of myogenin (red) localization in nuclei (blue) of CT, EV, and ICAM-1+ cells at 2 d of differentiation (scale bar = 100 μm). D) Quantitative analysis of myogenin localization, expressed as the percentage of nuclei expressing myogenin, through 3 d of differentiation (n=4). E) Quantitative analysis of creatine kinase activity through 3 d of differentiation (n=4). F) Representative western blot of phosphorylated (Thr180/Tyr182) p38 MAPK (P-p38) and total p38α (40 kDa) in CT, EV, and IC cells after 1–3 d of differentiation. G) Quantitative analysis of phosphorylated p38 MAPK levels through 3 d of differentiation (n=4).

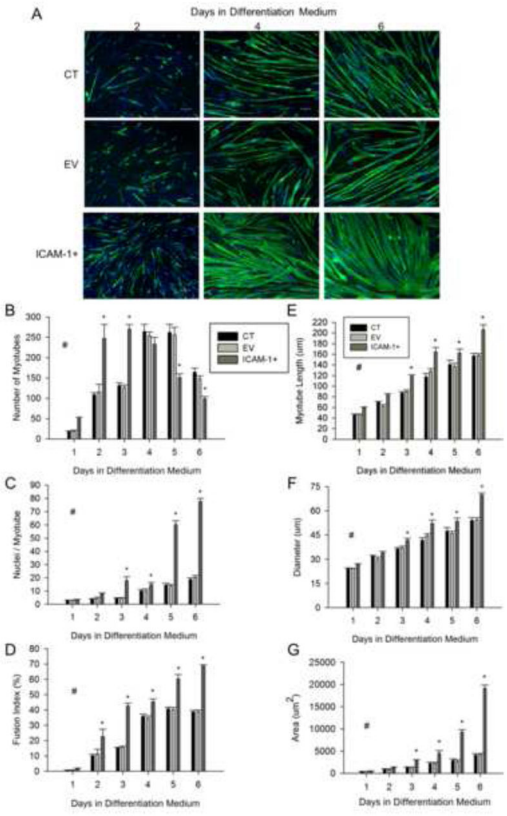

Figure 2.

Myotube formation, myonuclear number, and myotube size. A) Representative images of myosin heavy chain (green) and nuclei (blue) in control (CT), empty vector (EV), and ICAM-1+ cells at 2, 4, and 6 d of differentiation (scale bar = 100 μm). Quantitative analysis of myotube number (B), average number of nuclei within myotubes (C), fusion index (D), as well as myotube length (E), diameter (F), and area (G) through 6 d of differentiation (n=6). # = higher for ICAM-1+ compared to CT and EV cells throughout 6 d of differentiation (main effect for cell line; $p < 0.05$). * = different for ICAM-1+ compared to CT and EV cells at indicated day of differentiation (interaction effect; $p < 0.001$).

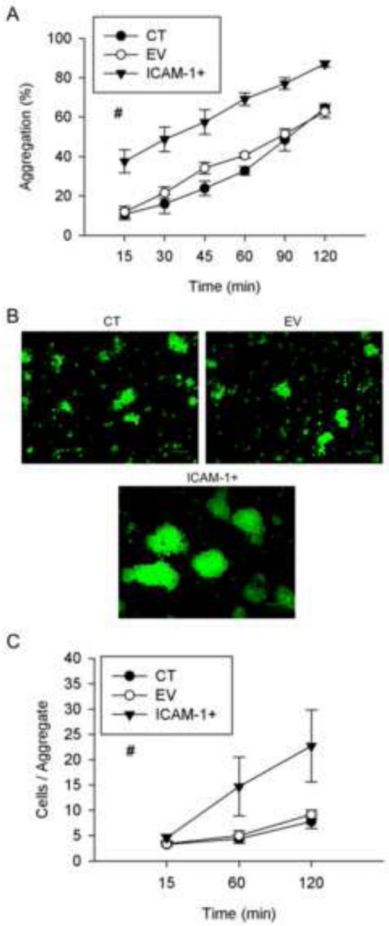

Figure 3.

Myoblast-myoblast adhesion. A) Percent aggregation of control (CT), empty vector (EV), and ICAM-1+ cells at selected intervals throughout 120 min of incubation (n=4–6). # = higher for ICAM-1+ compared to CT and EV cells (main effect for cell line; $p < 0.001$). B) Representative images of cytospin prepared slides of CT, EV, ICAM-1+ cells at 120 min of incubation (scale bar = 100 μm). Glutaraldehyde-induced fluorescence (green) was used to count the number of cells in individual aggregates. C) Average number of cells within aggregates of CT, EV, and ICAM-1+ cells at 15, 60, and 120 min of incubation (n=4–6). # = higher for ICAM-1+ compared to CT and EV cells (main effect for cell line; $p < 0.001$).

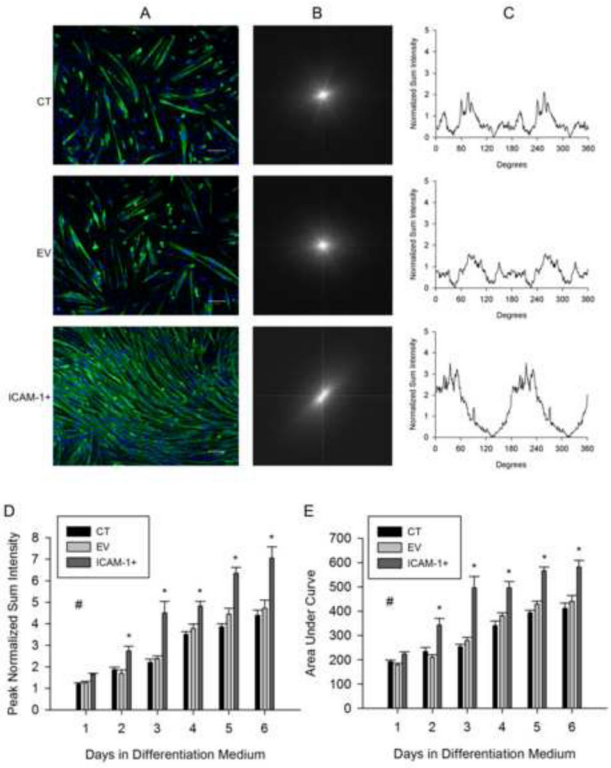

Figure 4.

Myotube alignment. A) Representative images of myosin heavy chain (green) and nuclei (blue) in control (CT), empty vector (EV), and ICAM-1+ cells at 3 d of differentiation (scale bar = 100 um). B) Representative fast Fourier transform (FFT) images of corresponding images of myosin heavy chain and nuclei. C) Corresponding FFT alignment plots showing normalized sum intensity on the y-axis and degrees (0–360) on the x-axis. Quantitative analysis of peak normalized sum intensity (D) and area under the curve (E) of the FFT alignment plots (n=6). # = higher for ICAM-1+ compared to CT and EV cells throughout 6 d of differentiation (main effect for cell line; $p < 0.001$). * = higher for ICAM-1+ compared to CT and EV cells at indicated day of differentiation (interaction effect; $p < 0.001$).

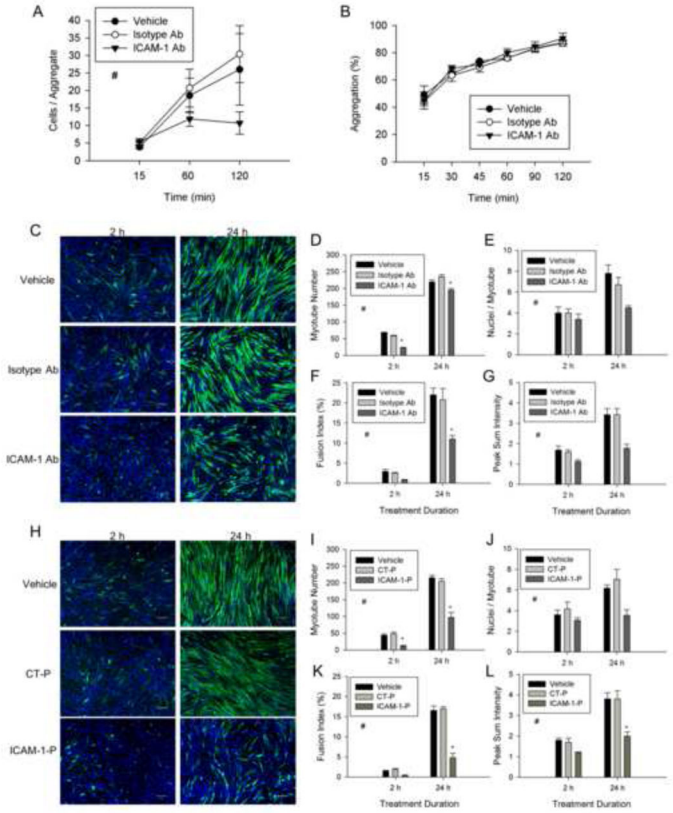

Figure 5.

The extracellular and cytoplasmic domains of ICAM-1 in the regulation of myotube formation, myonuclear accretion, and myotube alignment. ICAM-1+ cells were treated with vehicle, isotype control antibody (Isotype Ab; 100 μg/ml), control peptide (CT-P; 100 μg/ml), ICAM-1 antibody (ICAM-1 Ab; 100 μg/ml), or ICAM-1 peptide (ICAM-1-P; 100 μg/ml) at 1 d of differentiation for 2 or 24 h. A) Average number of cells within aggregates of ICAM-1+ cells treated with vehicle, Isotype Ab, or ICAM-1 Ab throughout 120 min of incubation (n=5). # = lower for ICAM-1 Ab compare to vehicle and Isotype-Ab (main effect for treatment; $p < 0.05$). B) Percent aggregation of ICAM-1+ cells treated with vehicle or antibody throughout 120 min of incubation (n=4). C) Representative images of myosin heavy chain (green) and nuclei (blue) in ICAM-1+ cells after 2 and 24 h treatment with vehicle or antibody (scale bar = 100 μm). Quantitative analysis of myotube number (D), average number of nuclei within myotubes (E), fusion index (F), and peak normalized sum intensity (G) (n=3). # = lower for ICAM-1 Ab compared to Isotype-Ab and vehicle (main effect for treatment; $p < 0.05$), * = lower for ICAM-1 Ab compared to Isotype-Ab and vehicle at indicated duration of treatment (interaction effect; $p < 0.05$). H) Representative images of myosin heavy chain (green) and nuclei (blue) in ICAM-1+ cells after 2 and 24 h treatment with vehicle or peptide (scale bar = 100 μm). Quantitative analysis of myotube number (I), average number of nuclei within myotubes (J), fusion index (K), and peak normalized sum intensity (L) (n=4). # = lower for ICAM-1-P compared to CT-P and vehicle (main effect for treatment; $p < 0.005$), * = lower for ICAM-1-P compared to CT-P and vehicle at indicated duration of treatment (interaction effect; $p < 0.05$).

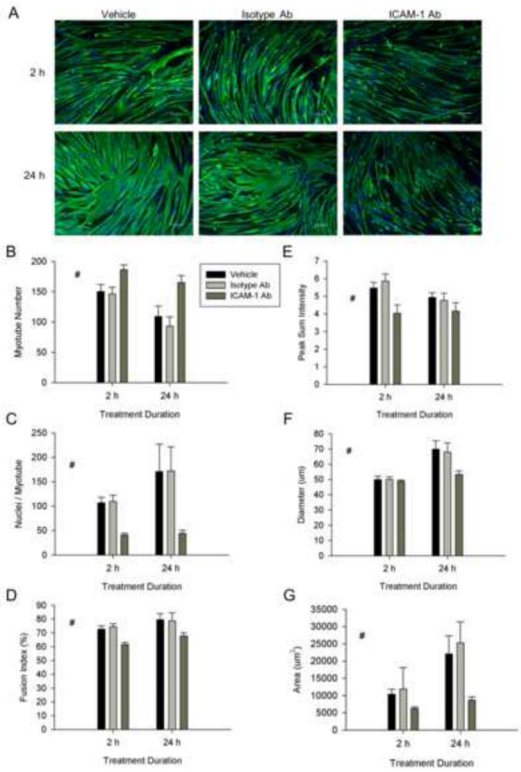

Figure 6.

The extracellular domain of ICAM-1 in the regulation of myotube fusion, alignment and size. ICAM-1+ cells were treated with vehicle, isotype control antibody (Isotype Ab;100 μg/ml), or ICAM-1 antibody (ICAM-1 Ab;100 μg/ml) at 5 d of differentiation for 2 or 24 h. A) Representative images of myosin heavy chain (green) and nuclei (blue) in ICAM-1+ cells after 2 and 24 h treatment with vehicle or antibody (scale bar = 100 μm). Quantitative analysis of myotube number (B), average number of nuclei within myotubes (C), and fusion index (D), as well as myotube alignment (E), diameter (F), and area (G) (n=4). # = different for ICAM-1 Ab compared to Isotype-Ab and vehicle (main effect for treatment; $p < 0.05$).

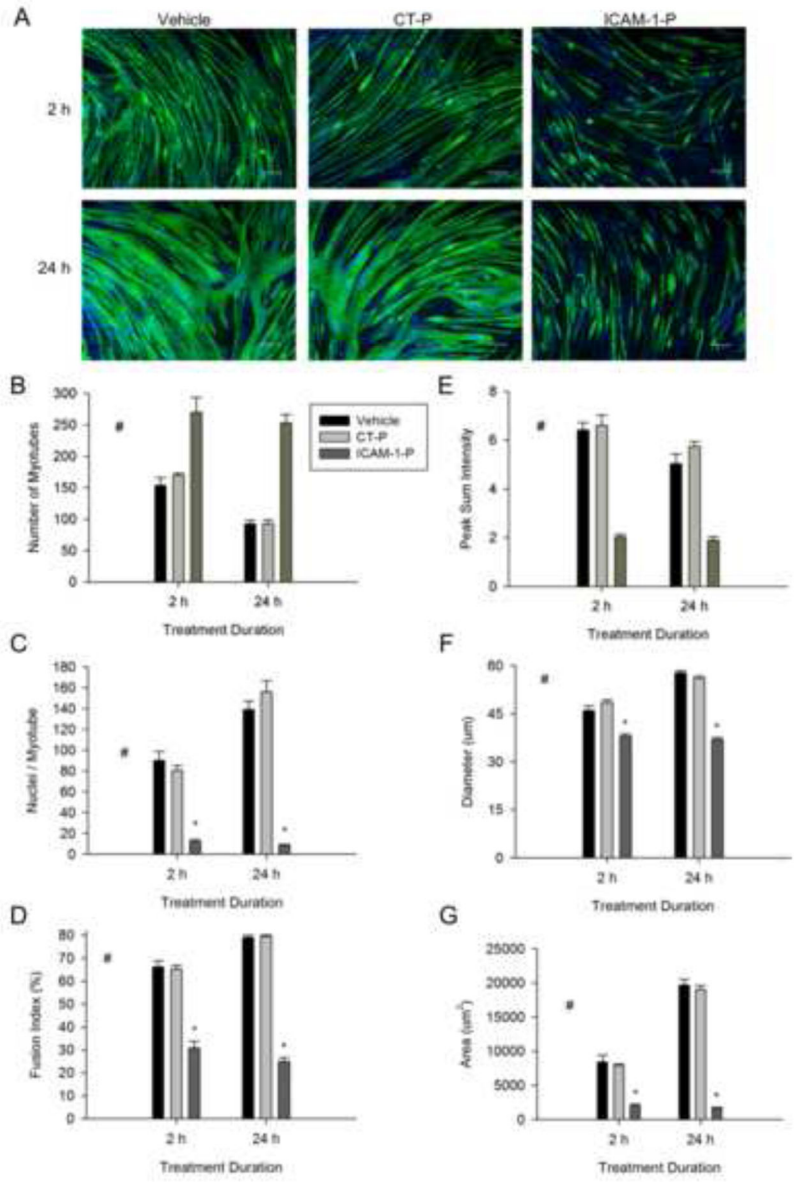

Figure 7.

The cytoplasmic domain of ICAM-1 in the regulation of myotube fusion, alignment and size. ICAM-1+ cells were treated with vehicle, control peptide (CT-P; 50 μg/ml) or ICAM-1 peptide (ICAM-1-P; 50 μg/ml) at 5 d of differentiation and myotube indices were quantified 2 and 24 h after treatment. A) Representative images of myosin heavy chain (green) and nuclei (blue) in ICAM-1+ cells after 2 and 24 h of treatment with vehicle, CT-P, and ICAM-1-P (scale bar = 100 μm). Quantitative analysis of myotube number (B), average number of nuclei within myotubes (C), and fusion index (D), as well as myotube alignment (E), diameter (F), and area (G) (n=4). # = different for ICAM-1-P compared to CT-P and vehicle (main effect for treatment; $p < 0.001$), * = lower for ICAM-1-P compared to CT-P and vehicle at indicated duration of treatment (interaction effect; $p < 0.001$).

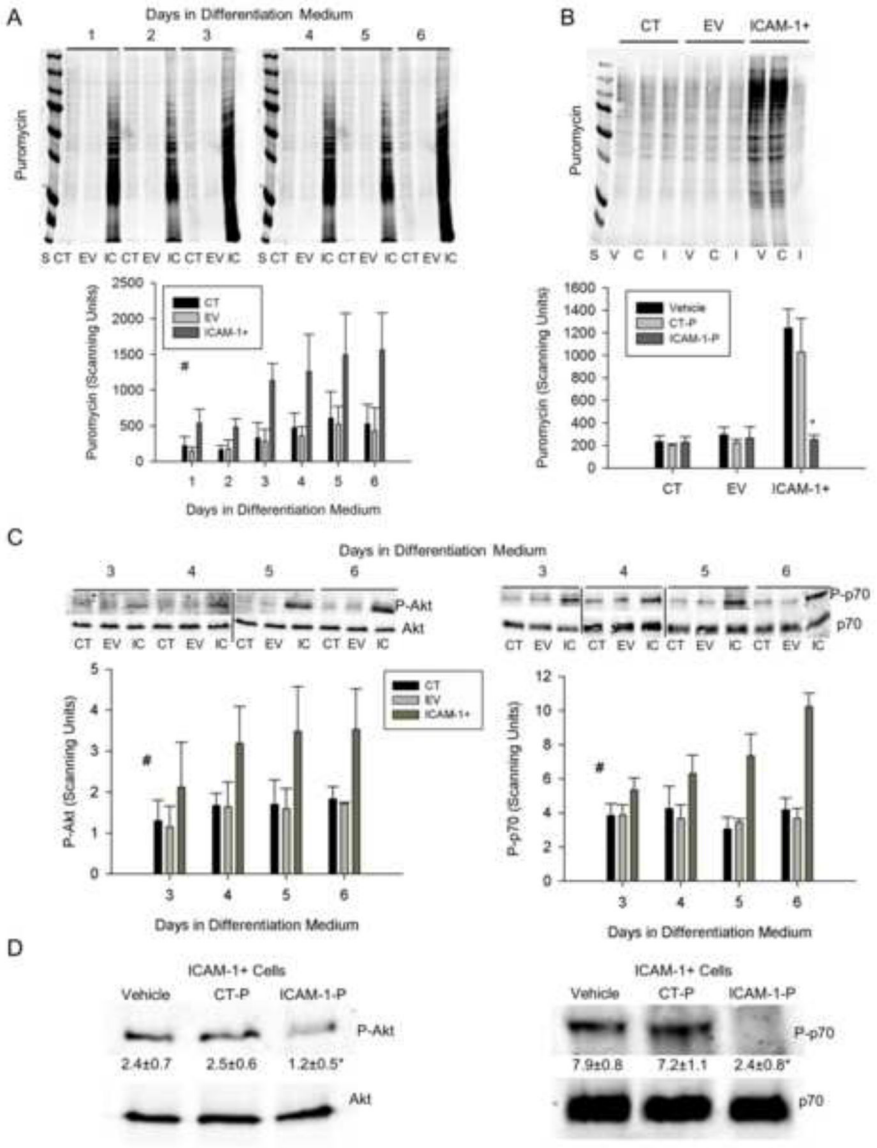

Figure 8.

Protein synthesis and Akt/p70s6k signaling. A) Representative western blot and quantitative analysis (n=4) of puromycin incorporation into nascent proteins of cells treated with differentiation medium for up to 6 d (25 μg/lane). S = standards (250-15 kDa), CT = control, EV = empty vector, IC = ICAM-1+. # = higher for ICAM-1+ compared to CT and EV cells throughout 6 d of differentiation (main effect for cell line; $p < 0.001$). B) Representative western blot and quantitative analysis (n=4) of puromycin in CT, EV and ICAM-1+ cells treated with vehicle (V), control peptide (C or CT-P; 50 μg/ml), or ICAM-1 peptide (I or ICAM-1-P; 50 μg/ml) at 5 d of differentiation for 2 h prior to collection of cell lysates. * = ICAM-1 peptide reduced protein synthesis in ICAM-1+ cells to levels that were observed in CT and EV cells (interaction effect; $p < 0.001$). C) Representative western blots of Akt and p70s6k, as well as quantitative analysis of phosphorylated Akt (Ser473; P-Akt) and p70s6k

(Thr389; P-p70) at 3–6 d of differentiation. # = higher for ICAM-1+ compared to CT and EV cells (main effect for cell line; $p < 0.005$). D) Representative western blots of Akt and p70s6k, as well as quantitative analysis of phosphorylated levels Akt and p70s6k for ICAM-1+ cells treated with vehicle, control peptide (CT-P; 50 μg/ml) or ICAM-1 peptide (ICAM-1-P; 50 μg/ml) at 5 d of differentiation for 2 h prior to collection of cell lysates. Scanning units are presented below blots for P-Akt and P-p70. * = lower for ICAM-1-P compared to vehicle and CT-P ($p < 0.05$).